PHYSICAL REVIEW LETTERS

VOLUME 43 | 5 NOVEMBER 1979 | NUMBER 19

Experimental Comparison of Neutrino, Antineutrino, and Muon Velocities

George R. Kalbfleisch
Fermi National Accelerator Laboratory, Batavia, Illinois 60510, and University of Oklahoma, Norman, Oklahoma 73019

and

Neil Baggett[a] and Earle C. Fowler
Purdue University, West Lafayette, Indiana 47907

and

Joshua Alspector
Bell Laboratories, Murray Hill, New Jersey 07974

(Received 4 June 1979)

No energy dependence of the velocities of neutrinos or antineutrinos is observed within the statistical and systematic errors over the energy range 30 to 200 GeV. The velocity differences (95% confidence level) are $|\beta_\nu - \beta_{\bar{\nu}}| < 0.7\times10^{-4}$, $|\beta_{\nu_K} - \beta_{\nu_\pi}| < 0.5\times10^{-4}$, and $|\beta_{\nu(\bar{\nu})} - \beta_\mu(\text{corrected})| = |\beta_{\nu(\bar{\nu})} - 1| < 0.4\times10^{-4}$, where $\beta = v/c$.

In Fermilab experiments[1,2] to measure the interaction cross sections of neutrinos and antineutrinos from pion decay (ν_π and $\bar{\nu}_\pi$) and from kaon decay (ν_K and $\bar{\nu}_K$), we have found that these neutrinos and antineutrinos have velocities which differ from those of energetic muons penetrating the shielding by no more than 1 part in 10^4 [95% confidence level (CL)]. Correcting for a systematic bias in the flight path of the penetrating muons we find that $|\beta_{\nu(\bar{\nu})} - 1| < 0.4\times10^{-4}$ (95% CL) from a sample of some 9800 events. This result is a factor of 10 improvement over our earlier result based on 100 events.[3] If neutrinos are indeed massless,[4] it is expected that they move at the speed of light.[5] However, since neutrinos are so vastly different from the other known particles, this expectation must be experimentally checked.[6] This paper reports the results of a significant test.

The experiment used the Fermilab narrow-band neutrino beam discussed several times previously (see, e.g., Ref. 2). The data come from neutrino runs with the momentum of the positive-hadron beam set to 80, 130, 190, and 250 GeV, and from antineutrino runs with the momentum of the negative-hadron beam set to 130, 190, and 230 GeV. Each run gives a sample of pion neutrinos and a sample of kaon neutrinos. For almost all of the data, time-of-flight information for the hadrons, the decay muons, and the neutrino and antineutrino interactions was recorded. We use the fact that the precise spacing of proton bunches in the accelerator yields 1-ns pulses of secondaries at intervals of 18.83 ns. If all products (secondaries from interactions, decays, etc.) travel with the same speed, this timing pattern is maintained. Our procedure is described in more detail in Ref. 3.

The velocity comparison of neutrinos and penetrating muons was obtained from temporally interleaved sets of data: the times of muons arising from neutrino interactions (events), and the times of muons penetrating the muon shield and the neutrino detector (decay muons). This local time comparison required an intermediate timing reference.

The experimental setup is shown schematically in Fig. 1. The 53.1-MHz rf signal from the accelerator was used as the primary intermediate reference. The time of the event (or decay muon) was measured by two counters, T3 and T2, imbedded in the detector. Two secondary timing references, MU and PI, were also used in order to understand the signal responses and the drifts and shifts which occurred during the 60-d data-taking period. The MU signal was obtained by combining together the signals from four of the eight fivefold muon telescopes located downstream of the secondary dump at the end of the 350-m decay space. The PI signal was obtained from a counter in the hadron beam coming through a small hole in this same dump.

Various timing combinations between the five signals, rf, MU, PI, T3, and T2, yield the intrinsic response and drift times given in Table I. For example, the MU-PI timing difference was stable as a function of time through the data taking. Also, the widths of T3-rf, T2-rf, and T3-T2 difference distributions determine the response times of T3 and T2 shown in Table I.

A number of shifts in the timing occurred due to changes in the accelerator tuning, electronic failures, and cabling. The data were sorted into chronological groups of data such that the energy of the beam and all of the time distributions remained consistent. 22 such groups resulted. The MU signal was absolutely stable. The T3 and T2 signals showed shifts after down times of the accelerator or the detector. Since the basic timing

TABLE I. Timing resolution.

Signal	σ_{response} (ns)	σ_{drift} (ns)
rf	$\lesssim 0.5$	$\lesssim 0.4$
MU	0.6–1.0	$\lesssim 0.2$
PI	1.6	0.3
T3	1.3	0.4
T2	1.0	0.6

technique is the local comparison (inside each of the 22 chronological and consistent sets of timing data) of the neutrino events relative to the penetrating muons, these shifts do not have any influence on the velocity differences. Any undetected shifts must be small and are covered in the deviations given in Table I.

In order to display the data in a uniform manner the average shift of each signal in each of the chronological groups from an arbitrarily chosen standard (channel 100 of time digitizer) was applied to the signals. In this way the various timing distributions may be summed and displayed over arbitrary subgroups of the data. The time difference of T2 relative to rf, for example, is nicely Gaussian out to 3 standard deviations as shown in Fig. 2.

The means and standard deviations of the various timing distributions are computed for each neutrino energy (ν_π, $\bar{\nu}_\pi$, ν_K, and $\bar{\nu}_K$), for the closed momentum-slit (wide-band background) runs, and for the dimuon sample.[7] The corresponding velocity differences averaged over (T3-rf) and (T2-rf) can then be computed as presented in Table II. These differences are also shown in Fig. 3, plotted against the average neutrino energy $\bar{E}_{\nu,\bar{\nu}}$. Note that all the velocity differences $\beta_{\nu(\bar{\nu})} - \beta_\mu$ are positive and nonzero. This effect is interpreted as a bias due to the fact that the penetrating muons travel a slightly longer distance from target to detector, because of multi-

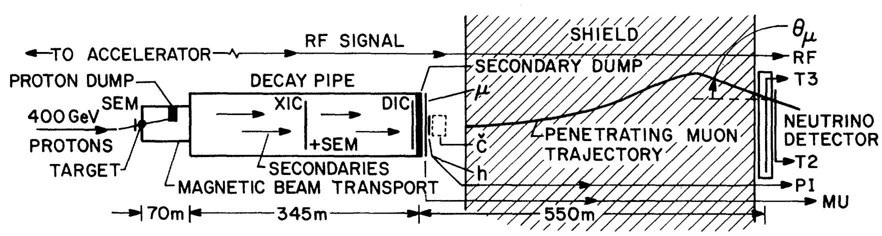

FIG. 1. The experimental layout. 400-GeV protons incident on an aluminum target form secondary beams of pions, kaons, and other particles. The neutrinos and a few energetic muons penetrate the shield in front of the detector. The five timing signals, rf, MU, PI, T3, and T2, arise from the detectors indicated. Also shown in a representative trajectory of a decay muon in the shield and its angle (θ_μ) in the neutrino detector.

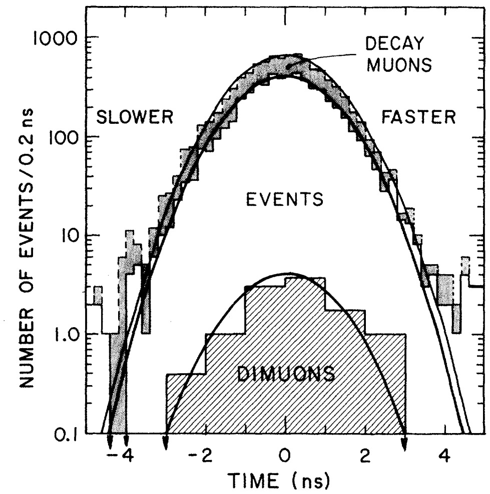

FIG. 2. Timing distributions of the T2 signals relative to the rf signal for about 40% of the "events" (open area), "decay muons," and a sample of "dimuons." (The outer histogram is the sum of events and decay muons.) The curves drawn through the data are Gaussians centered on zero time with a standard deviation of of 1.1 ns.

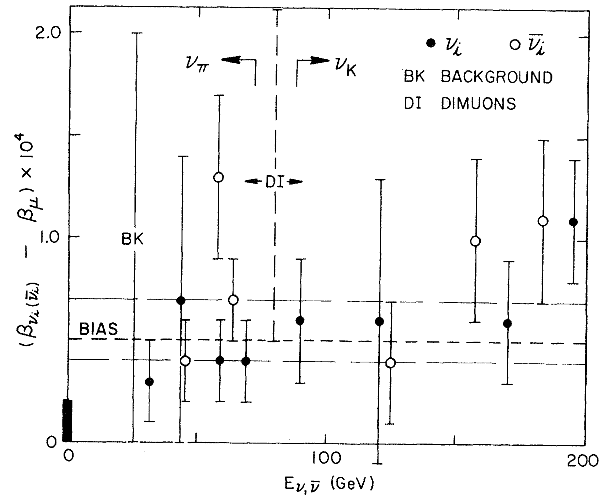

FIG. 3. The neutrino (antineutrino) minus penetrating-muon velocity differences of Table II vs neutrino energy $E_{\nu,\bar\nu}$. The dashed line and shaded area represent the estimated timing bias of the penetrating muon due to multiple scattering in the shield. The dark vertical bar at the origin represents the maximum possible bias due to other sources.

ple scattering, than the straight-line path of the neutrinos. This bias is estimated below to be $(+0.5^{+0.2}_{-0.1}) \times 10^{-4}$ and is shown as the dashed line and shaded region in Fig. 3.

The penetrating muons have a mean energy of about 30 GeV exiting from the decay shield. The mean muon energy entering the shield is about 200 GeV. At the lower energy settings, the pen-

TABLE II. Velocity Differences.

Sample	$\bar{E}_{\nu_i}$ (GeV)	Neutrino events	Decay muons	$\beta_\nu\beta_\mu$ (10^{-4})
+ 80 ν_π	32	1480	1998	0.3 ± 0.2
+130 ν_π	44	476	46	0.7 ± 0.7
−130 $\bar\nu_\pi$	45	437	639	0.4 ± 0.2
+190 ν_π	59	2085	1037	0.4 ± 0.2
−190 $\bar\nu_\pi$	58	1223	1505	1.3 ± 0.4
+250 ν_π	69	906	1102	0.4 ± 0.2
−230 $\bar\nu_\pi$	64	782	2723	0.7 ± 0.2
+ 80 ν_K	90	303	1998	0.6 ± 0.3
+130 ν_K	120	121	46	0.6 ± 0.7
−130 $\bar\nu_K$	125	195	639	0.4 ± 0.3
+190 ν_K	170	1015	1037	0.6 ± 0.2
−190 $\bar\nu_K$	157	225	1505	1.0 ± 0.4
+250 ν_K	195	519	1102	1.1 ± 0.3
−130 $\bar\nu_K$	183	112	2723	1.1 ± 0.4
Background	26	38	150	1.0 ± 0.1
Dimuons	30–200	65[a]	9050	1.3 ± 0.8
Bias $(1-\beta_\mu)$	$\bar{E}_\mu = 23$–37	⋯	⋯	$0.5^{+0.2}_{-0.1}$
All $\lvert\beta_{\nu(\bar\nu)} - 1\rvert$	⋯	9879	9050	< 0.4[b] (95% CL)
All $\lvert\beta_\mu - \beta_{\bar\nu}\rvert$	⋯	6905/2974	9050	< 0.7 (95% CL)
All $\lvert\beta_{\nu_K} - \beta_{\nu_\pi}\rvert$	⋯	2490/7286	9050	< 0.5 (95% CL)

[a]One is a trimuon. [b]Corrected for bias (see text).

etrating muons arise from the small high-momentum tail of the beam momentum distribution. Multiple scattering of the muons in the shield corresponds to that of an average energy of 80 GeV. A possible muon trajectory is sketched in Fig. 1. The muons scatter to some mean radius from the central beam line near the end of the decay shield. A small fraction of these muons receive a large multiple scattering back towards the detector. The mean square angle, $\langle\theta^2\rangle^{1/2}$, for the penetrating decay muons as observed in the detector is 0.024 to 0.032 rad.[8] Extrapolating the average muon trajectory in the detector back into the shielding along the mean angles, we find that they intersect the mean multiple-scattered trajectories from the target about 100 to 120 m from the downstream end of the shield at a radius of about 3 m. This radius is about the same size as the width of the shield. The muon flight path along this trajectory is then some 0.03 to 0.06 m longer than a straight-line path to the detector and corresponds to the estimated bias given above. We see in Fig. 3 that the data points overlap with the shaded region. The other possible bias, the velocity difference of the muons with respect to light, is negligible in comparison with the above.[9] We assume that charged muons behave as expected from special relativity.[10]

The data of Table II and Fig. 3 appear to show a (linear) rise with increasing neutrino energy $E_{\nu,\bar{\nu}}$. A best-fit line is $(0.3\pm0.1)+(0.003\pm0.001)E_\nu$ parts per 10^4. A higher-order polynomial would give a less significant slope parameter. Thus we take the data to be consistent with a constant value. Correcting for the bias, we obtain, averaging over energy, the additional entries in Table II,

$$|\beta_{\nu(\bar{\nu})}-\beta_\mu(\text{corrected})| = |\beta_{\nu(\bar{\nu})}-1| < 0.4\times10^{-4}\ (95\%\ \text{CL}),$$

$$|\beta_{\nu_K}-\beta_{\nu_\pi}| < 0.5\times10^{-4}\ (95\%\ \text{CL}),$$

and

$$|\beta_\nu-\beta_{\bar{\nu}}| < 0.7\times10^{-4}\ (95\%\ \text{CL}).$$

The dimuon subsample is also in agreement with these values and thus consistent with the interpretation that they mainly arise from neutrino interactions (charm production and/or pion or kaon decays) rather than some slow ($\beta<1$) heavy-lepton source. Unfortunately no timing information is available for neutral-current events.

It is a pleasure to acknowledge the support of Fermilab and its staff, and of our home institutions. We thank our California Institute of Technology–Fermilab–Rockefeller University collaborators, and especially Professor Frank Sciulli, for allowing us to extend our earlier analysis[3] into other neutrino and antineutrino samples, and for supplying us with the identity of the events in the dimuon sample. This work was supported by the U. S. Department of Energy.

[(a)]Currently at Division of High Energy Physics, U. S. Department of Energy, Washington, D. C. 20545.

[1]G. R. Kalbfleisch *et al.*, in *Neutrinos—78*, edited by E. C. Fowler (Purdue Univ. Press, W. Lafayette, Ind., 1978), p. 951.

[2]B. C. Barish *et al.*, Phys. Rev. Lett. 39, 1595 (1977).

[3]J. Alspector *et al.*, Phys. Rev. Lett. 36, 837 (1976).

[4]Mass limits for ν_π, see E. V. Schrum and K. O. H. Ziock, Phys. Lett. 37B, 114 (1971), and G. Backentoss *et al.*, Phys. Lett. 43B, 539 (1973); and for ν_k, see A. R. Clark *et al.*, Phys. Rev. D 9, 533 (1974).

[5]Apart from a possible very slight difference in the effective indices of refraction experienced by photons and neutrinos passing through empty space, due to their differing (electromagnetic versus weak) interactions with fluctuations of the physical vacuum.

[6]G. R. Kalbfleisch, Brookhaven National Laboratory Informal Report No. 20227 (unpublished); see also Z. G. T. Guiragossián *et al.*, Phys. Rev. Lett. 34, 335 (1975).

[7]Only 65 of the 119 dimuons and trimuons [B. C. Barish *et al.*, Phys. Rev. Lett. 39, 981 (1977)] fall in our fiducial region and data cuts mentioned in the text.

[8]The (T3 and T2) times of the muons in the detector were corrected for the observed angle of the actual trajectories (about 0.02 ns on average).

[9]The expected bias due to the observed $\bar{E}_\mu \gtrsim 30$ GeV corresponds to $1-\beta_\mu \lesssim 6\times10^{-6}$.

[10]Upper limits on the deviation of the velocity of electrons, pions, kaons, and protons from the expectations of special relativity are discussed in Ref. 6. In addition, a conservative limit on the muon velocity can be inferred from the differential Cherenkov studies of the composition of the hadron beams in our experiment. The "muon" pressure curve is found to be essentially identical to the pion curve. These muons (mostly from pion decay) have a momentum > 0.5 that of the pions. For the 80-GeV hadron setting, the muons have $1-\beta \lesssim 4\times10^{-6}$ from the "muon" pressure curve obtained in this experiment (not published). This is to be compared with $1-\beta<3\times10^{-6}$ expected for $E_\mu>40$ GeV.